

Pinning control of chimera states in systems with higher-order interactions

Riccardo Muolo,^{1,*} Lucia Valentina Gambuzza,² Hiroya Nakao,^{1,3} and Mattia Frasca^{2,4}

¹*Department of Systems and Control Engineering, Tokyo Institute of Technology, Tokyo 152-8552, Japan*

²*Department of Electrical, Electronics and Computer Science Engineering, University of Catania, 95125 Catania, Italy*

³*International Research Frontiers Initiative, Tokyo Institute of Technology, Kanagawa 226-8501, Japan*

⁴*Istituto di Analisi dei Sistemi ed Informatica "A. Ruberti", IASI-CNR, 00185 Roma, Italy*

(Dated: September 5, 2024)

Understanding and controlling the mechanisms behind synchronization phenomena is of paramount importance in nonlinear science. In particular, chimera states, patterns in which order and disorder coexist simultaneously, continue to puzzle scholars, due to their elusive nature. Recently, it has been shown that higher-order interactions greatly promote the onset of chimera states, which are easier to find and more resilient when the system units interact in group. In this work, we show that the higher-order framework is fertile not only for the emergence of chimera states, but also for their control. Via pinning control, a technique consisting in applying a forcing to a subset of the nodes, we are able to trigger the emergence of chimera states with only a small fraction of controlled nodes, at striking contrast with the case without higher-order interactions. We show that our setting is robust for different higher-order topologies and types of pinning control and, finally, we give a heuristic interpretation of the results via phase reduction theory. Our numerical and theoretical results provide further understanding on how higher-order interactions shape nonlinear dynamics.

Keywords Chimera states, pinning control, higher-order interactions, synchronization, hypergraphs

I. INTRODUCTION

Understanding the mechanisms underlying self-organization phenomena on networks is a paramount task in the study of complex systems, which is complemented by the development of efficient methods to control such dynamics [1]. This is particularly relevant in the framework of synchronization dynamics, where, depending on the applications, it is fundamental to achieve a synchronized state, e.g., in power grids [2], or to break it into an asynchronous one, e.g., in neuroscience [3], where synchronization is often associated to pathological states. The network framework remains still relevant in the modeling of complex systems, nonetheless, over the past years scholars have started considering more complex structures such as hypergraphs and simplicial complexes [4–8]. This is because networks do not capture interactions beyond the pairwise setting, i.e., two-by-two, while many systems have shown evidence of higher-order, i.e., group, interactions [4, 5]. Examples come from, but are not limited to, neuroscience [9–12], ecology [13, 14] and social behaviors [15]. Higher-order interactions have been proven to greatly affect the collective behavior, for instance, in random walks [16, 17], synchronization dynamics [18–20], contagion [21] and pattern formation [22, 23], to name just a few. Given the ubiquity of group interactions [4–8], it is important to understand how to control the dynamics in such systems. While significant progress has been made in the control of networks [24, 25], the investigation into the control of systems with higher-order interactions has only recently begun [26–29].

The focus of this work is an intriguing type of synchronization pattern called chimera state, which consists of the coexistence of coherent and incoherent domains of oscillations. Coexistence of coherence and incoherence was first observed by Kaneko for globally coupled chaotic maps [30] and was then found in several numerical settings with global [31–33] and nonlocal [34–38] coupling schemes. Despite all the previous research on the subject, the work that historically is considered to be the first to characterize the emergence of chimera states is the well-known paper by Kuramoto and Battogtokh [39], made popular by a successive work of Abrams and Strogatz, who, with a creative intuition, compared the coexistence of different dynamical state to the chimera, a mythological creature in which parts of different animals coexisted [40]. Besides the pure theoretical relevance of such an astonishing phenomenon, a great part of the interest has been generated by the existence of analogous patterns in real systems: for instance, in Josephson junctions [41] and electronic circuits [42, 43], laser [44], mechanical [45] and nano-electromechanical systems [46], to name a few. Particular attention has been devoted to neuroscience [47, 48], specifically to unihemispheric sleeping patterns in animals [49]. Except for some particular configurations in which robust chimera patterns are induced by the network structure [50, 51], in both numerical and experimental settings chimera states are often elusive and characterized by a rather short lifetime. Hence, there is a vast literature on networked systems, consisting in looking for different settings (e.g., parameter ranges, network topologies, coupling configurations, etc.) making such patterns easier to find and with a longer lifetime. Moreover, after the first definition by Kuramoto and Battogtokh [39], several kinds of chimera states have been defined, e.g., amplitude chimeras [52] or phase chimeras [53]. We will not thoroughly discuss such studies, inviting the interested reader to consult a book [54] and a review [55] on the subject. In the context of higher-order interactions, chimera states have

* corresponding author: muolo.r.aa@m.titech.ac.jp

been proven to be enhanced in some pioneering works considering both pairwise and higher-order interactions [56–58]. This claim was further corroborated in [59] for systems with pure higher-order interactions, where the emergence of chimera states on higher-order topologies is compared with the absence of such patterns when the interactions are pairwise.

In this work, we consider the setting studied in [59] and implement a control to further trigger the emergence of chimera states. Our control approach will rely on the so called *pinning control*, a technique used to drive networks onto a desired dynamical state by using a control input applied to a small subset of nodes [60, 61]. Such technique has been successfully used in the framework of opinion dynamics [62, 63], epidemics [64, 65], pattern formation [66] and synchronization dynamics [67–69], to name a few. The latter includes the control of chimera states with pairwise interactions, which we hereby extend to the higher-order framework. Indeed, in [69] it was shown that it is possible to trigger the emergence of chimera states via pinning. Nonetheless, to achieve such task, at least half of the network nodes need to be controlled. In what follows, after introducing the setting in Sec. II, we show that higher-order interactions considerably facilitate the work of the controllers and chimera states can be obtained by controlling only a small fraction of the nodes. Such results are shown in Sec. III for two different kinds of pinning approaches, that we named additive pinning and parametric pinning. Moreover, we show that, rather than the number of nodes, what matters is the size of the hyperedges, i.e., the group of nodes interacting with each other. Then, before the discussion of some potential future directions, we give a heuristic interpretation of the results based on the phase reduction theory [70] in Sec. IV.

II. THE MODEL AND THE SETTING

In this Section, we introduce the system exhibiting chimera states, which is analogous to that studied in [59]. We consider coupled Stuart-Landau oscillators, a paradigmatic model for the study of synchronization dynamics, given that it is the normal form of the supercritical Hopf-Andronov bifurcation [71]. The coupling takes place through pure higher-order interactions, namely, by mean of a higher-order topology called *nonlocal hyperring*, which is a generalization of the nonlocal pairwise coupling [59]. The type of chimera state that we will hereby consider is that of *phase chimeras*, states have been first observed by Zajdela and Abrams [53], which consist in oscillation patterns where the amplitude and the frequency of each oscillator are the same, but the phases exhibit a chimera behavior, i.e., a part of the oscillators have the same phase, while the other phases are distributed along the unit circle. The peculiarity of such pattern is that, once obtained, it does not vary, because the frequency is the same for all the oscillators. Hence, we would observe the same exact pattern after each period. For this reason, we find the description given by Zajdela and Abrams, "frozen patterns of disorder", perfectly fitting. The reader can find a thorough characterization of these patterns in the Refs. [53, 59]. On a side, let us note that multitailed phase chimeras have only been found in the pairwise setting [53], but not yet in the higher-order one. In what follows, every chimera state discussed and shown in the figures will be a phase chimera. For sake of simplicity, we will refrain from using the word "phase" and will call them simply "chimeras".

A. Stuart-Landau oscillators coupled via nonlocal hyperrings

We consider a system made of N interacting Stuart-Landau units. In the absence of any interaction, each unit i of the system is described by the following equations

$$\begin{cases} \dot{x}_i = \alpha x_i - \omega y_i - (x_i^2 + y_i^2) x_i = f(x_i, y_i), \\ \dot{y}_i = \omega x_i + \alpha y_i - (x_i^2 + y_i^2) y_i = g(x_i, y_i), \end{cases} \quad (1)$$

where α is a bifurcation parameter and ω is the frequency of the oscillators. Let us stress that the units are homogeneous, meaning that the parameters α and ω are the same for each and every system. Each isolated system exhibits a stable limit cycle for $\alpha > 0$, which is the case we will consider throughout this study.

To model the higher-order interactions we use a generalization of the links (or edges) called *hyperedges*, whose structure can be encoded by using *adjacency tensors*, a generalization of the adjacency matrices for networks [4]. From the literature dealing with simplicial complexes [6], we adopt the convention that a hyperedge of $(d + 1)$ nodes (i.e, encoding a $(d + 1)$ -body interaction) is called a d -hyperedge. As an example, let us consider the 3-rd order¹ adjacency tensor (i.e., encoding 4-body interactions) $A^{(3)} = \{A_{ijkl}^{(3)}\}$. We have that $A_{ijkl}^{(3)} = 1$ if nodes i, j, k, l are part of the same hyperedge and 0 otherwise. This is

¹ Let us note that in tensor algebra the order (or rank) of a tensor is given by its indices, e.g., a scalar is a 0-rank tensor, a vector is a 1-rank tensor, a matrix is a 2-rank tensor, etc. Hence, $A^{(3)} = \{A_{ijkl}^{(3)}\}$ would be a 4-rank tensor and the adjacency matrix, given that it is a matrix, a 2-rank tensor. However, here we follow that notation that is most commonly used in the literature on higher-order interactions.

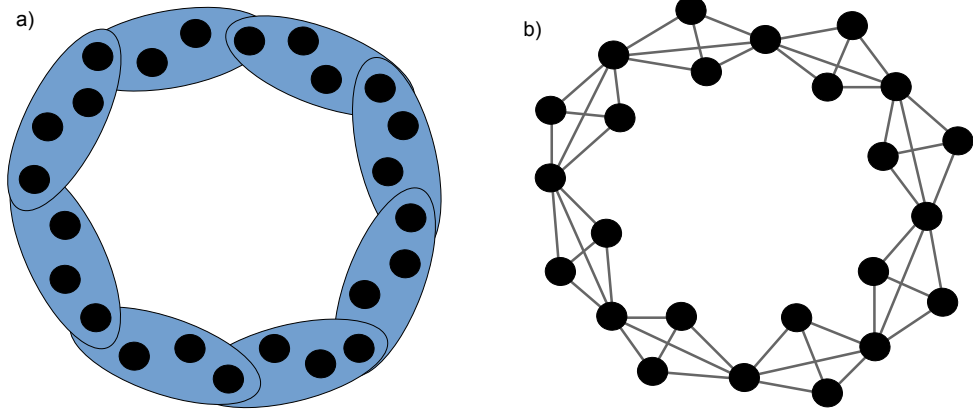


Figure 1. In panel a), a 3-hyperring of 24 nodes, together with its corresponding clique-projected network, depicted in panel b). We will call the nodes which are part of two hyperedges (resp. cliques) *junction nodes*, while all the others will be called *non-junction nodes*.

the analogous of the adjacency matrix for networks, which is, indeed, a 1-st order adjacency tensor. The chosen higher-order topology is that of *nonlocal d -hyperrings*, a pure higher-order structure introduced in [59] and consisting of hyperedges of size $d + 1$ (d is the order of the interaction) attached through one node and set in a circular structure. In Fig. 1, we depict a 3-hyperring, in panel a), together with its pairwise counterpart, namely, the *clique-projected network (cpn)* obtained by projecting each hyperedge into a clique having the same size, in panel b). Observe that a hyperring is a uniform hypergraph, the hyperedges all having the same size.

Following the analyses carried out in previous works [43, 59], we assume the coupling to involve only the first state variable of each oscillator, i.e., x . Let us stress that other coupling configurations can be considered, as discussed in Appendix A. With the above assumption, the equations for systems (1) coupled via a generic d -hyperring read

$$\begin{cases} \dot{x}_i = f(x_i, y_i) + \varepsilon \sum_{j_1, \dots, j_d=1}^N A_{i, j_1, \dots, j_d}^{(d)} (h^{(d)}(x_{j_1}, \dots, x_{j_d}) - h^{(d)}(x_i, \dots, x_i)), \\ \dot{y}_i = g(x_i, y_i) + \varepsilon \sum_{j_1, \dots, j_d=1}^N A_{i, j_1, \dots, j_d}^{(d)} (h^{(d)}(x_{j_1}, \dots, x_{j_d}) - h^{(d)}(x_i, \dots, x_i)), \end{cases} \quad (2)$$

where $\varepsilon > 0$ is the coupling strength². Because we consider identical oscillators, together with the fact that the coupling is diffusive like, i.e., it vanishes when all oscillators are in the same state, system (2) admits a fully synchronous solution. Such a coupling is a special type of non-invasive interaction [72]. Moreover, we will consider coupling functions such that the higher-order interaction cannot be decomposed into pairwise ones³. Eq. (2) can be rewritten in compact form for each unit i as

$$\dot{\vec{X}}_i = \vec{F}(\vec{X}_i) + \mathbb{D} \sum_{j_1, \dots, j_d=1}^N A_{i, j_1, \dots, j_d}^{(d)} (\vec{H}^{(d)}(\vec{X}_{j_1}, \dots, \vec{X}_{j_d}) - \vec{H}^{(d)}(\vec{X}_i, \dots, \vec{X}_i)), \quad (3)$$

where $\vec{X}_i = (x_i, y_i)^\top$, $\vec{F} = (f, g)^\top$, $\vec{H}^{(d)} = (h^{(d)}, h^{(d)})^\top$ and $\mathbb{D} = \varepsilon D = \varepsilon \begin{bmatrix} 1 & 0 \\ 1 & 0 \end{bmatrix}$. As stated previously, in Appendix A we report additional results for different coupling matrices D .

To highlight the effects of higher-order interactions, we will perform a comparison between the dynamics on the hyperring and

² Note that such configuration involves only interactions of order d , i.e., $(d + 1)$ -body, hence it is not necessary to denote the coupling strength with ε_d .

³ It was shown by Neuhäuser et al. that the higher-order coupling functions need to be nonlinear, otherwise the many-body interaction can be decomposed into pairwise ones [73]. Successively, it was further shown that such assumption may not be enough and, if the nonlinear functions h are the sum of nonlinear terms which separately account for each unit, e.g., $h^{(d)}(x_{j_1}, \dots, x_{j_d}) = h(x_{j_1}) + \dots + h(x_{j_d})$, they can still be decomposed into pairwise ones [23].

on its respective clique-projected network (cpn), as in [59]. The equations for the dynamics with pairwise interactions are

$$\begin{cases} \dot{x}_i = f(x_i, y_i) + \varepsilon \sum_{j=1}^N A_{i,j}^{(1)} (h^{cpn}(x_j) - h^{cpn}(x_i)), \\ \dot{y}_i = g(x_i, y_i) + \varepsilon \sum_{j=1}^N A_{i,j}^{(1)} (h^{cpn}(x_j) - h^{cpn}(x_i)), \end{cases} \quad (4)$$

where the coupling functions for the dynamics on the clique-projected network h^{cpn} is determined from its corresponding $h^{(d)}$ (see below).

We will perform pinning control on hyperrings of 4 different orders, namely, 3-,4-,5- and 6-hyperrings, involving 4-,5-,6- and 7-body interactions, respectively. In line with other previous works, e.g., [72], we will consider odd-degree polynomials as coupling functions. The coupling functions for each hyperring and its clique-projected network are the following

$$\begin{cases} h^{(3)}(x_{j_1}, x_{j_2}, x_{j_3}) = x_{j_1} x_{j_2} x_{j_3} & , \quad h^{cpn}(x_j) = x_j^3, \\ h^{(4)}(x_{j_1}, x_{j_2}, x_{j_3}, x_{j_4}) = x_{j_1}^2 x_{j_2} x_{j_3} x_{j_4} & , \quad h^{cpn}(x_j) = x_j^5, \\ h^{(5)}(x_{j_1}, x_{j_2}, x_{j_3}, x_{j_4}, x_{j_5}) = x_{j_1} x_{j_2} x_{j_3} x_{j_4} x_{j_5} & , \quad h^{cpn}(x_j) = x_j^5, \\ h^{(6)}(x_{j_1}, x_{j_2}, x_{j_3}, x_{j_4}, x_{j_5}, x_{j_6}) = x_{j_1}^2 x_{j_2} x_{j_3} x_{j_4} x_{j_5} x_{j_6} & , \quad h^{cpn}(x_j) = x_j^7, \end{cases} \quad (5)$$

where the adjacency tensor accounts for all the permutations of the indexes. As an example, let us explicit the equations for the 4-body case (3-hyperring) and its corresponding clique-projected network. The equations for a 3-hyperring are the following

$$\begin{cases} \dot{x}_i = \alpha x_i - \omega y_i - (x_i^2 + y_i^2) x_i + \varepsilon \sum_{j_1, j_2, j_3}^N A_{i, j_1, j_2, j_3}^{(3)} (x_{j_1} x_{j_2} x_{j_3} - x_i^3), \\ \dot{y}_i = \omega x_i + \alpha y_i - (x_i^2 + y_i^2) y_i + \varepsilon \sum_{j_1, j_2, j_3}^N A_{i, j_1, j_2, j_3}^{(3)} (x_{j_1} x_{j_2} x_{j_3} - x_i^3), \end{cases} \quad (6)$$

while those for the clique-projected network are

$$\begin{cases} \dot{x}_i = \alpha x_i - \omega y_i - (x_i^2 + y_i^2) x_i + \varepsilon \sum_j^N A_{i,j} (x_j^3 - x_i^3), \\ \dot{y}_i = \omega x_i + \alpha y_i - (x_i^2 + y_i^2) y_i + \varepsilon \sum_j^N A_{i,j} (x_j^3 - x_i^3). \end{cases} \quad (7)$$

The equations for interactions of different orders can be constructed analogously by means of the coupling functions (5) (see also the SM of [59]).

B. Hyperedge-based local order parameter

To quantify the synchronization of an ensemble of oscillators it is common to use the Kuramoto order parameter [74], which gives a global measure of how much the oscillators are synchronized. However, chimera states involve the coexistence of coherent (i.e., synchronized) and incoherent (i.e., desynchronized) oscillators and the respective regions are localized. Hence, a global measure of the synchronization does not provide useful information on the chimera state. For this reason, scholars have proposed a *local* Kuramoto order parameter, which measures the synchronization in a given region of the network, by quantifying the differences between neighboring oscillators, as was done, for instance, in [69]. In the case of hyperrings, a

natural extension of the local order parameter would need to account for the synchronization inside each hyperedge rather than some arbitrary neighborhood. Partially inspired by a work by Shanahan [75], where the order parameter is defined with respect to the communities of a network, we hereby define a *hyperedge-based local order parameter* as follows:

$$\mathcal{R}_i^{\mathcal{E}}(t) = \left| \frac{1}{\mathcal{E}_i} \sum_{j \in \mathcal{E}_i} e^{i\vartheta_j(t)} \right|, \quad (8)$$

where i is the imaginary unit, ϑ_j is the (time evolving) phase of the j -th oscillator and \mathcal{E}_i is the hyperedge(s) node i is part of. By taking as example a 3-hyperring, Fig. 1a), we can see that, if node i is a junction node, then it is part of 2 different hyperedges and will have 6 neighboring nodes, while non-junction nodes will have only 3 neighbors. From that, we can observe that non-junction nodes will have the same hyperedge-based local order parameter $\mathcal{R}_i^{\mathcal{E}}$. The number of nodes with the same $\mathcal{R}_i^{\mathcal{E}}$ in each hyperedge increases with the order of the hyperring: for instance, in 3-hyperrings they will be 2, while in 6-hyperrings they will be 5.

In analogy with the hyperedge-based local order parameter, for the clique-projected network we define a clique-based local order parameter as follows

$$\mathcal{R}_i^{\mathcal{C}}(t) = \left| \frac{1}{C_i} \sum_{j \in C_i} e^{i\vartheta_j(t)} \right|, \quad (9)$$

where C_i is the clique(s) node i is part of.

C. Pinning control

Chimera states are often elusive patterns, emerging only for limited ranges of the parameters and specific initial conditions [54]. Higher-order interactions greatly enhance the possibility of observing such a behavior [57, 59, 76]. Nonetheless, *ad hoc* initial conditions remain a fundamental prerequisite for the chimera to emerge. Our goal is, hence, to induce chimera states in settings where they would not spontaneously appear. For this, we put to use a popular technique in control theory, called pinning control, which consists in externally acting on a subset of the nodes to drive the dynamics of the whole ensemble of nodes towards a desired state [60, 61], and has been successfully applied in the context of chimera states on networks [69]. In our setting, the pinning will act as a perturbation on a subset of the nodes, with the goal of developing a region of incoherence, while leaving the unperturbed nodes in their synchronous state.

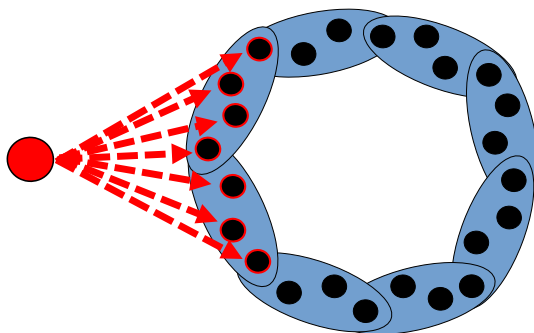


Figure 2. Scheme of the pinning control for a 3-hyperring of 24 nodes. The system starts in the synchronized state and the control input is applied to a subset of the nodes to induce the emergence of a chimera state.

In order to implement the control, we need to determine which nodes to pin and for how much time. Hence, let us define the pinning time t_p , i.e., the time during which the control will be active, and the number of pinned nodes, $N_p < N$. We will denote all the nodes with the index $i = 1, \dots, N$ and the subset of pinned nodes with $i_p = 1, \dots, N_p$. Let us observe that, in the context of pairwise interactions, a chimera state is obtained when about half of the nodes are controlled [69]. In Sec. III, where we show the numerical results, the reader will appreciate the great advantage offered by the presence of higher-order interactions. The pinning control setting is schematically depicted in Fig. 2.

1. Control protocol I: additive pinning control

Let us now proceed with setting up the control protocol. The first type of pinning control is called *additive*, and it was successfully implemented in [69] to control chimera states with pairwise interactions. In such a setting, the pinned nodes receive an input in an additive fashion. The equations read

$$\dot{\vec{X}}_i = \vec{F}(\vec{X}_i) + \mathbb{D} \sum_{j_1, \dots, j_d=1}^N A_{i, j_1, \dots, j_d}^{(d)} \left(\vec{H}(\vec{X}_{j_1}, \dots, \vec{X}_{j_d}) - \vec{H}^{(d)}(\vec{X}_i, \dots, \vec{X}_i) \right) + \vec{U}_i, \quad (10)$$

where $\vec{U}_i = \vec{0}$ for non controlled nodes and, for $i = i_p$, $\vec{U}_{i_p} = (u_{i_p}(t), u_{i_p}(t))^\top$, with

$$u_{i_p}(t) = \lambda_{i_p} [\Theta(t) - \Theta(t - t_p)], \quad (11)$$

where λ_{i_p} are parameters drawn from a uniform distribution of a given interval and Θ is the Heaviside step function, whose value is 1 when the argument is positive and 0 when it is null or negative. This way, the control is active as long as $t \leq t_p$.

2. Control protocol II: parametric pinning control

The second type of pinning control we are going to implement consists in acting on the controlled nodes by modifying the parameters of the dynamical system. This protocol, which we will call *parametric pinning control*, is given by the following equations

$$\dot{\vec{X}}_i = \vec{F}_i(\vec{X}_i) + \mathbb{D} \sum_{j_1, \dots, j_d=1}^N A_{i, j_1, \dots, j_d}^{(d)} \left(\vec{H}(\vec{X}_{j_1}, \dots, \vec{X}_{j_d}) - \vec{H}^{(d)}(\vec{X}_i, \dots, \vec{X}_i) \right), \quad (12)$$

where $\vec{F}_i = \vec{F}$ for the nodes that are not pinned, while, for $i \equiv i_p = 1, \dots, N_p$, it is given by $\vec{F}_i = (f_{i_p}, g_{i_p})^\top$, where

$$\begin{cases} f_{i_p}(x_{i_p}, y_{i_p}) = \alpha x_{i_p}(t) - \Omega_{i_p}(t) y_{i_p}(t) - (x_{i_p}^2(t) + y_{i_p}^2(t)) x_{i_p}(t), \\ g_{i_p}(x_{i_p}, y_{i_p}) = \Omega_{i_p}(t) x_{i_p}(t) + \alpha y_{i_p}(t) - (x_{i_p}^2(t) + y_{i_p}^2(t)) y_{i_p}(t). \end{cases} \quad (13)$$

The frequency of the controlled nodes, $\Omega_{i_p}(t)$, is given by

$$\Omega_{i_p}(t) = \omega \Theta(t - t_p) + \omega_{i_p} \Theta(t_p - t), \quad (14)$$

where ω_{i_p} is new frequency induced by the pinning and Θ is the Heaviside step function, whose value is 1 when the argument is positive and 0 when it is null or negative. This ensures that $\Omega_{i_p} = \omega_{i_p}$ for $t \leq t_p$ and it switches to ω as soon as the control is switched off. In our numerical implementation, the new frequencies ω_{i_p} will be drawn from a uniform distribution of a given positive interval. As a last remark, let us note that the control acts only on the frequency and not on the amplitude, because we have numerically verified that acting on the amplitude has no effect whatsoever.

III. NUMERICAL RESULTS

In this section we show the numerical results of our pinning approaches. We start by comparing the case of a 3-hyperring, where chimera states occur with both pinning approaches, with its corresponding clique-projected network, where chimera states do not emerge. Then, we will exploit the hyperring structure and develop a pinning strategy that maximizes the width of the incoherence region while the number of controlled nodes remains low. For the latter, we will show the results only for additive pinning, leaving the discussion of the analogous results obtained through parametric pinning in Appendix B.

A. Comparison between higher-order and pairwise interactions

Let us proceed in testing our pinning approaches to control the emergence of chimera states on a 3-hyperring and compare it with the clique-project network case. In Figs. 3 and 4, we show the results for the additive pinning on a hyperring and a clique-projected network, respectively, while, in Figs. 5 and 6, we show the results for the parametric pinning on a hyperring and a clique-projected network, respectively. For both pinning approaches, we see that the control induces a chimera state when the topology is higher-order (Figs. 3 and 5). Moreover, such state persists for long integration times⁴. These features can be visualized through the hyperedge-induced local order parameter $\mathcal{R}_i^{\mathcal{E}}$, which shows that the nodes which have been controlled are not oscillating coherently with respect to their neighbors sharing the same hyperedge(s) and that such incoherence persists. On the other hand, the pairwise case does not yield chimeras (Figs. 4 and 6). In fact, the initial decoherence induced by the control is quickly reabsorbed by the system and, although a clear trace of the pinning remains, the difference between the phases of adjacent oscillators is small and the variation smooth. This can be visualized through the clique-based order parameter $\mathcal{R}_i^{\mathcal{C}}$. Note that in [59] the latter state was distinguished from a chimera one through the total phase variation. Our approach based on a local order parameter is complementary.

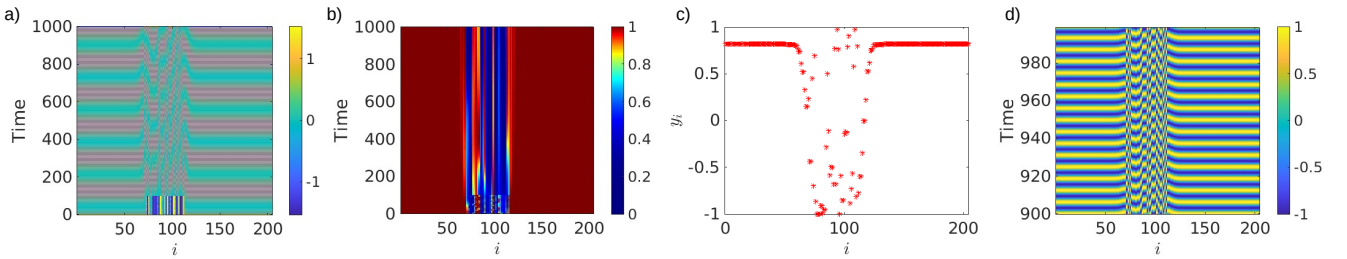


Figure 3. Additive pinning induces phase chimera states on a 3-hyperring (i.e., 4-body interactions) of 204 nodes. Panel a) depicts the whole time series of variables $y_i(t)$ with $i = 1, \dots, N$, panel b) the hyperedge-based local order parameter, panel c) a snapshot of variables $y_i(t)$ with $i = 1, \dots, N$ for $t_{final} = 1000$ time units and panel d) shows a zoom of the time series of variables $y_i(t)$ with $i = 1, \dots, N$. The model parameters are $\alpha = 1$ and $\omega = 1$ and the coupling strength is $\varepsilon = 0.01$. Pinning control is applied to $N_p = 40$ consecutive nodes for $t_p = 100$ time units. The parameters λ_{ip} are drawn from a uniform distribution in the interval $[-2, 2]$.

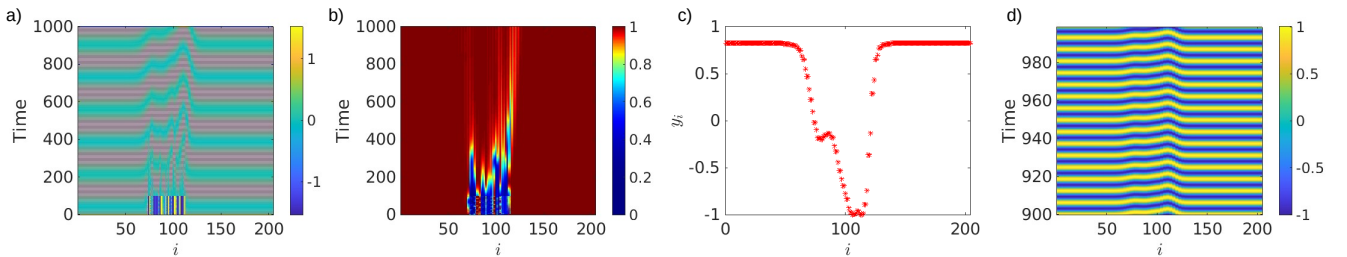


Figure 4. Additive pinning on a clique-projected network of 204 nodes. Chimera states do not emerge in this setting, at contrast with the previous Fig. 3. Panel a) depicts the whole time series of variables $y_i(t)$ with $i = 1, \dots, N$, panel b) the clique-based local order parameter, panel c) a snapshot of variables $y_i(t)$ with $i = 1, \dots, N$ for $t_{final} = 1000$ time units and panel d) shows a zoom of the time series of variables $y_i(t)$ with $i = 1, \dots, N$. The model parameters are $\alpha = 1$ and $\omega = 1$ and the coupling strength is $\varepsilon = 0.01$. Pinning control is applied to $N_p = 40$ consecutive nodes for $t_p = 100$ time units. The parameters λ_{ip} are the same of the previous figure.

Additionally, let us stress that all results hereby shown, regardless of the order of the hyperring, coupling and pinning approach, are due to the higher-order topology and no chimera states are found when performing the simulations with the same setting but on the corresponding clique-projected network, exactly as in the figures shown in this section. Note, though, that there is one particular exception discussed in Appendix A, where the observed pattern is not due to the higher-order topology but due to the coupling configuration, and, in fact, it is found also in the corresponding pairwise system. Such results provide further evidence that higher-order interactions promote the presence of chimera states and are consistent with the existing literature [57, 59, 76].

⁴ In the figures, we show the temporal evolution until 1000 time steps, while the chimera persists until about 4000 time steps. After such integration time, the chimera state turns into an incoherent state where variation between adjacent phases is smooth, but $\mathcal{R}_i^{\mathcal{E}}$ is low. We have found this state to persist with constant $\mathcal{R}_i^{\mathcal{E}}$ until 20000 time steps (the maximum integration time tested).

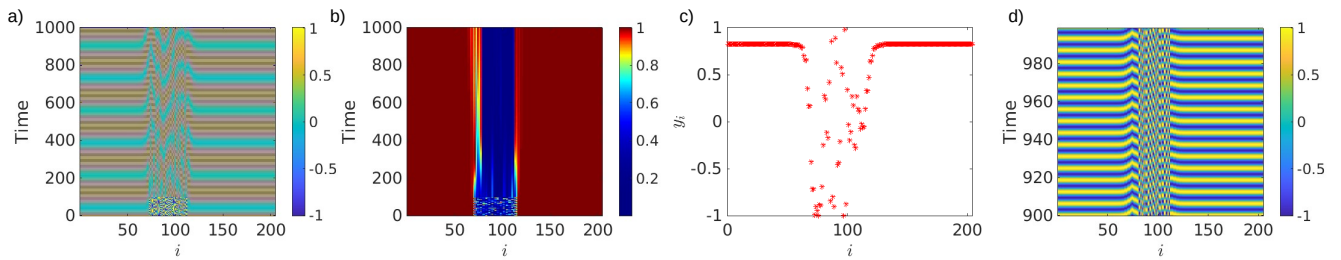


Figure 5. Parametric pinning induces phase chimera states on a 3-hyperring (i.e., 4-body interactions) of 204 nodes. Panel a) depicts the whole time series of variables $y_i(t)$ with $i = 1, \dots, N$, panel b) the hyperedge-based local order parameter, panel c) a snapshot of variables $y_i(t)$ with $i = 1, \dots, N$ for $t_{final} = 1000$ time units and panel d) shows a zoom of the time series of variables $y_i(t)$ with $i = 1, \dots, N$. The model parameters are $\alpha = 1$ and $\omega = 1$ and the coupling strength is $\varepsilon = 0.01$. Pinning control is applied to $N_p = 40$ consecutive nodes for $t_p = 100$ time units. The parameters ω_{i_p} are drawn from a uniform distribution in the interval $[0.5, 2.5]$.

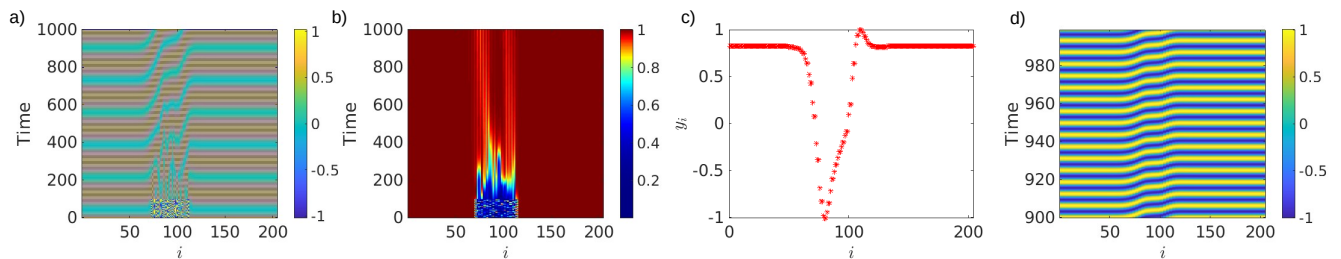


Figure 6. Parametric pinning on a clique-projected network of 204 nodes. Chimera states do not emerge in this setting, at contrast with the previous Fig. 5. Panel a) depicts the whole time series of variables $y_i(t)$ with $i = 1, \dots, N$, panel b) the clique-based local order parameter, panel c) a snapshot of variables $y_i(t)$ with $i = 1, \dots, N$ for $t_{final} = 1000$ time units and panel d) shows a zoom of the time series of variables $y_i(t)$ with $i = 1, \dots, N$. The model parameters are $\alpha = 1$ and $\omega = 1$ and the coupling strength is $\varepsilon = 0.01$. Pinning control is applied to $N_p = 40$ consecutive nodes for $t_p = 100$ time units. The parameters ω_{i_p} are the same of the previous figure.

Let us conclude by pointing out that in previous works chimera states were obtained for specific values of the initial conditions, while random or uniform initial conditions did not yield the same result. In our numerical study, the initial conditions do not matter as long as the system starts on the synchronous solution, i.e., on the limit cycle of the Stuart-Landau oscillator (1). Hence, we will choose the initial conditions to be uniform and without noise, i.e., $(x_j^0 = 1, y_j^0 = 0)$ for every oscillator.

B. Scaling of the pinned subset with respect to the hyperring size

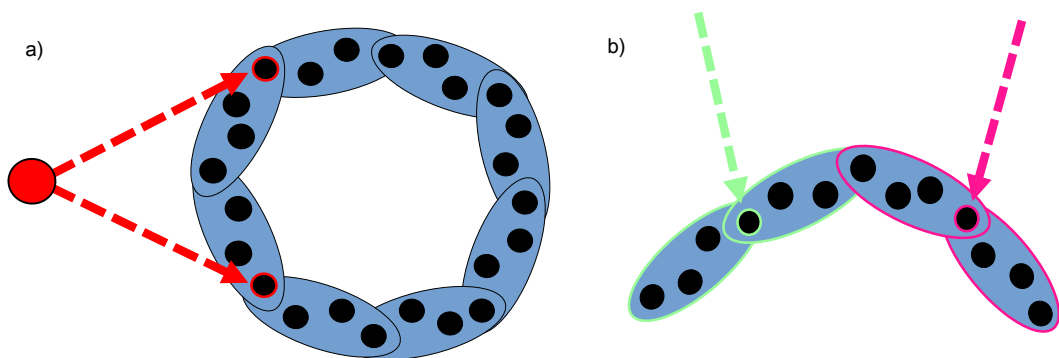


Figure 7. Pinning scheme allowing us to exploit the structure of the hyperring. In panel a), we show a setting in which we can, in principle, control half of the nodes while pinning only 2 nodes. In panel b), it is schematically shown how a control of the junction node affects two hyperedges. Such protocol, shown for a 3-hyperring, is straightforwardly extended to any d -hyperring.

It is already remarkable that the higher-order framework favors the onset of chimera states with respect the pairwise one, but here we also show that the percentage of nodes required to obtain a chimera state, by exploiting the interactions of the hyperring, is small. Hence, we set up a pinning protocol in which we try to maximize the number of nodes affected by one single controller. Due to the hyperring structure, a way can be to pin every other junction node, so that each controlled node can, in principle, affect two hyperedges, as schematically shown in Fig. 7. To observe how the number of pinned nodes scales with the size of the hyperring, we keep constant the number of hyperedges, so that the total number of nodes increases, but the backbone of the structure remains unchanged. Given that each pinned node is part of 2 hyperedges, in principle, we are able to control all the nodes in these hyperedges. E.g., in a 3-hyperring, with each pinned nodes we would control 7 nodes, in a 4-hyperring 9 nodes, in a 5-hyperring 11 nodes and in a 6-hyperring 13 nodes. For brevity, we present here the results for the additive pinning. The results for the parametric pinning are similar and can be found in Appendix B.

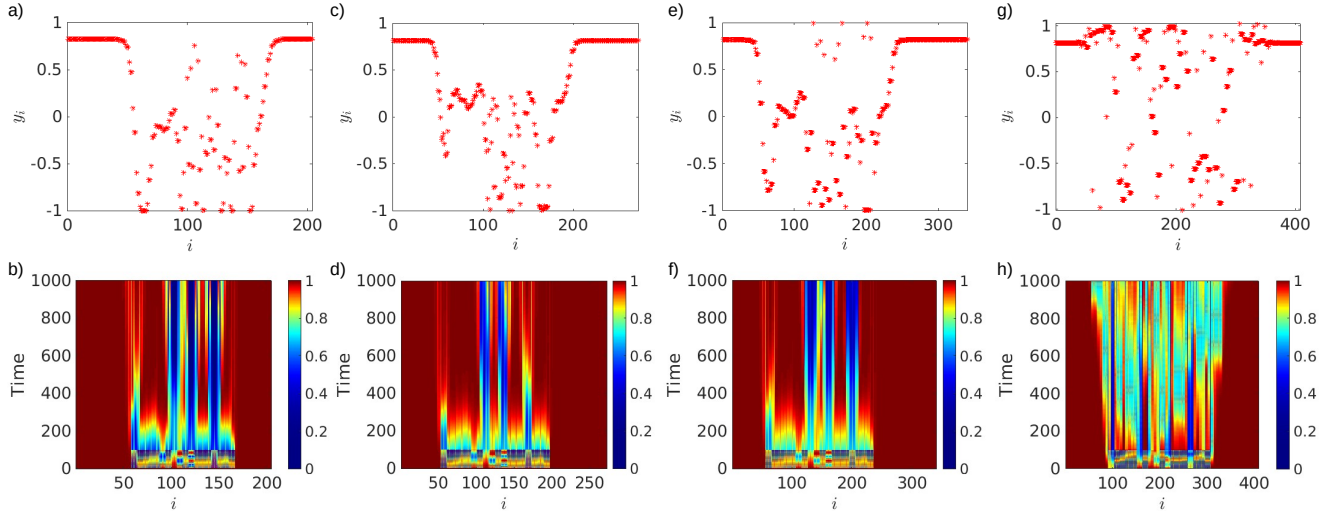


Figure 8. Scaling of the pinned subset with respect to the higher-order structure size with the additive pinning approach. On the upper panels we depict the snapshots of variables $y_i(t)$ with $i = 1, \dots, N$ for $t_{final} = 1000$ time units, while the lower panels show the hyperedge-based local order parameters. Panels a) and b) report the simulations performed on a 3-hyperring (i.e., 4-body interactions) of 204 nodes, panels c) and d) on a 4-hyperring (i.e., 5-body interactions) of 272 nodes, panels e) and f) on a 5-hyperring (i.e., 6-body interactions) of 340 nodes and panels g) and h) on a 6-hyperring (i.e., 7-body interactions) of 408 nodes. The number of nodes is chosen so that each hyperring is made of 68 hyperedges. Pinning control is applied to $N_p = 18$ nodes as in Fig. 7, i.e., every two junction nodes, to all the structures and for $t_p = 100$ time units. This means that the pinned nodes are $\approx 8.8\%$ of the total nodes in the 3-hyperring, $\approx 6.6\%$ of the total nodes in the 4-hyperring, $\approx 5.3\%$ of the total nodes in the 5-hyperring and $\approx 4.4\%$ of the total nodes in the 6-hyperring. The model parameters are $\alpha = 1$ and $\omega = 1$, the coupling strength is $\varepsilon = 0.01$, except for the 6-hyperring where $\varepsilon = 0.1$, and the parameters λ_{i_p} are drawn from a uniform distribution in the interval $[0, 2]$ and are the same for all the simulations.

In Fig. 8, we show the results obtained with such control scheme on d -hyperrings with $d = 3, 4, 5, 6$, i.e., 4-, 5-, 6- and 7-body interactions, where we have fixed the number of hyperedges. Indeed, we can observe that we obtain a chimera state by inducing a large region of incoherence (more than half of the nodes) with a control that involves only a small fraction of the nodes. Moreover, the pinned nodes N_p are kept constant for every structure, meaning that N_p does not scale with the number of nodes, but rather with the number of hyperedges, which allows to control large structures with only a handful of nodes. The pinned nodes are $\approx 8.8\%$ of the total nodes for the 3-hyperring (panels a) and b)), $\approx 6.6\%$ of the total nodes for the 4-hyperring (panels c) and d)), $\approx 5.3\%$ of the total nodes in the 5-hyperring (panels e) and f)) and $\approx 4.4\%$ of the total nodes in the 6-hyperring (panels g) and h)). In the latter case, our pinning scheme does not work as well as for the other structures and the coupling strength need to be significantly increased in order to observe a chimera state. However, we can observe from Fig. 8h) that the chimera is not anymore stable and the front of incoherence enlarges. Let us stress that stable chimera states can be easily obtained also in 6-hyperrings by reducing the distance between the controlled nodes, as in the previous section, instead of the pinning scheme of Fig. 7.

Let us note that the parameters λ_{i_p} need to be all positive or all negative in order for this pinning scheme to yield persistent chimera states. When such random inputs are drawn in a symmetric interval with respect to the 0, e.g., $[-2, 2]$ as in Fig. 3, a chimera states forms but vanishes at about 400 time units. On the other hand, when the control inputs have the same sign, e.g., $[0, 2]$ as in Fig. 8, the chimera is persistent until about 4000 time units, i.e., 10 times longer.

In Appendix B, we show analogous results for the parametric pinning, except for the case 6-hyperring, where chimera states do not emerge by pinning every other junction node, even with stronger couplings. The fact that our results are robust with

respect to different control approaches is a good indication of the pervasiveness of the phenomenon.

Let us conclude the Results Section by pointing out that the chimera behavior can be further enhanced by increasing the number of pinned nodes and/or reducing the distance between them. Moreover, by increasing the magnitude of the parameters λ_{i_p} , we can also obtain chimera states through controlling even less nodes than in the simulations hereby shown. However, we have presented a setting in which the parameters λ_{i_p} have a magnitude comparable with the involved parameters, in order to make it suitable for applications.

IV. HEURISTIC INTERPRETATION THROUGH PHASE REDUCTION THEORY

In this section we will give a heuristic interpretation of the results based on the phase reduction approach [70, 77], which consists of reducing a given oscillatory system to a phase, i.e., Kuramoto-type, model [74]. In a nutshell, starting from a system of N highly dimensional units in a limit cycle regime, e.g.,

$$\dot{\vec{X}}_i = \vec{F}_i(\vec{X}_i) + \varepsilon \sum_{j=1}^N A_{ij} \vec{G}_{ij}(\vec{X}_j, \vec{X}_i), \quad (15)$$

under given assumptions (see [70] for details), we can reduce to a system of N interacting phase oscillators of the form

$$\dot{\vartheta}_i = \omega_i + \varepsilon \sum_{j=1}^N A_{i,j} \vec{Z}(\vartheta_i) \cdot \vec{G}_{ij}(\vartheta_j, \vartheta_i), \quad (16)$$

where ω_i is the frequency of the i -th oscillator and \vec{Z} is the phase sensitivity function. The key in the reduction process is to find an expression for \vec{Z} , which has an analytical expression only for some specific cases, among which the Stuart-Landau model [70] and weakly nonlinear oscillators [78], while it needs to be obtained numerically for general oscillators.

The phase reduction theory has been applied also to systems with higher-order interactions [79–81], obtaining higher-order versions of the Kuramoto model, which exhibit much richer behaviors than the pairwise one. Indeed, the first evidence of higher-order-induced exotic behaviors, which triggered the interest of the community towards this new framework, has come from higher-order phase models (although not derived through phase reduction) [18–20, 82, 83]. In what follows, we will apply the phase reduction to our model on a 3-hyperring and on the corresponding clique-projected network, Eqs. (6) and (7) respectively, to give an intuition of why it is easier to induce chimera behavior via pinning when the topology is higher-order. For the Stuart-Landau model, the phase sensitivity function is $\vec{Z}(\vartheta) = (-\sin(\vartheta), \cos(\vartheta))^T$ [70]. Let us consider system (6) in polar coordinates, i.e., $\vec{X}_i = (\cos(\vartheta_i), \sin(\vartheta_i))$, and proceed with the reduction by computing the following

$$\begin{aligned} \vec{Z}(\vartheta_i) \cdot \dot{\vec{X}}_i &= \sin^2(\vartheta_i) \dot{\vartheta}_i + \cos^2(\vartheta_i) \dot{\vartheta}_i = \\ &= -\alpha \cos(\vartheta_i) \sin(\vartheta_i) + \omega \sin^2(\vartheta_i) + \cos(\vartheta_i) \sin(\vartheta_i) + \omega \cos^2(\vartheta_i) + \alpha \cos(\vartheta_i) \sin(\vartheta_i) - \cos(\vartheta_i) \sin(\vartheta_i) + \\ &+ \varepsilon \sum_{j_1, j_2, j_3}^N A_{i, j_1, j_2, j_3}^{(3)} \left(\cos^3(\vartheta_i) \sin(\vartheta_i) - \cos(\vartheta_{j_1}) \cos(\vartheta_{j_2}) \cos(\vartheta_{j_3}) \sin(\vartheta_i) + \cos(\vartheta_{j_1}) \cos(\vartheta_{j_2}) \cos(\vartheta_{j_3}) \cos(\vartheta_i) - \cos^4(\vartheta_i) \right), \end{aligned}$$

which gives

$$\dot{\vartheta}_i = \omega + \varepsilon \sum_{j_1, j_2, j_3}^N A_{i, j_1, j_2, j_3}^{(3)} \Phi(\vartheta_i, \vartheta_{j_1}, \vartheta_{j_2}, \vartheta_{j_3}), \quad (17)$$

where

$$\Phi(\vartheta_i, \vartheta_{j_1}, \vartheta_{j_2}, \vartheta_{j_3}) = \cos^3(\vartheta_i) \sin(\vartheta_i) - \cos(\vartheta_{j_1}) \cos(\vartheta_{j_2}) \cos(\vartheta_{j_3}) \sin(\vartheta_i) + \cos(\vartheta_{j_1}) \cos(\vartheta_{j_2}) \cos(\vartheta_{j_3}) \cos(\vartheta_i) - \cos^4(\vartheta_i). \quad (18)$$

Observe that ω is the same for all the oscillators because we started from identical Stuart-Landau systems. If we apply the same procedure to the system on the clique-projected network, i.e., Eq. (7), we obtain

$$\dot{\vartheta}_i = \omega + \varepsilon \sum_j^N A_{i,j} \Psi(\vartheta_i, \vartheta_j), \quad (19)$$

where

$$\Psi(\vartheta_i, \vartheta_j) = (\cos(\vartheta_i) - \sin(\vartheta_i))(\cos^3(\vartheta_j) - \cos^3(\vartheta_i)). \quad (20)$$

Through the averaging method [70], the 4-body coupling (18) can be approximated as

$$\Phi(\vartheta_i, \vartheta_{j_1}, \vartheta_{j_2}, \vartheta_{j_3}) \simeq \frac{3}{8} \left(\sin(\vartheta_{j_1} + \vartheta_{j_2} + \vartheta_{j_3} - 3\vartheta_i) + \cos(\vartheta_{j_1} + \vartheta_{j_2} + \vartheta_{j_3} - 3\vartheta_i) - 1 \right), \quad (21)$$

while the pairwise coupling as (20)

$$\Psi(\vartheta_i, \vartheta_j) \simeq \frac{3}{8} \left(\sin(\vartheta_j - \vartheta_i) + \cos(\vartheta_j - \vartheta_i) - 1 \right) = \sqrt{2} \frac{3}{8} \sin\left(\vartheta_j - \vartheta_i + \frac{\pi}{4}\right) - \frac{3}{8}. \quad (22)$$

The coupling given by Eq. (22) steers the system towards synchronization, because $\Psi(\vartheta_i, \vartheta_j)$ has form of the well-known Kuramoto-Sakaguchi coupling, i.e., $\sin(\vartheta_j - \vartheta_i + \alpha)$, which is known to be attractive for $|\alpha| < \frac{\pi}{2}$ [84]. On the other hand, Eq. (21) allows for a much richer dynamics, given that there are many more combinations of the phases and the coefficients such that the coupling term vanishes, as it is the case of the higher-order Kuramoto model [81]. This fact, gives an intuition not only of the much richer dynamics observed when higher-order interactions are present [18–20, 81, 83], but also of why higher-order systems favor the presence of chimera states and it is much easier to induce such behavior via pinning, compared to the pairwise case. Moreover, given the form of the higher-order coupling terms, once such state is achieved, it is more difficult for the higher-order system to steer towards synchronization, which provides a qualitative explanation of why the chimera states are also persistent. Let us remark that the first intuition of this behavior was given by Zhang et al. in [85], where it was shown, for the higher-order Kuramoto model, that, when the systems leaves the attraction basin of the synchronous state, it is more difficult to synchronize again because higher-order interactions cause a shrinking of such attraction basin, which becomes smaller. In our case, the control pushes the system away from the synchronous solution creating a chimera state and the higher-order interactions favor the persistence of this state.

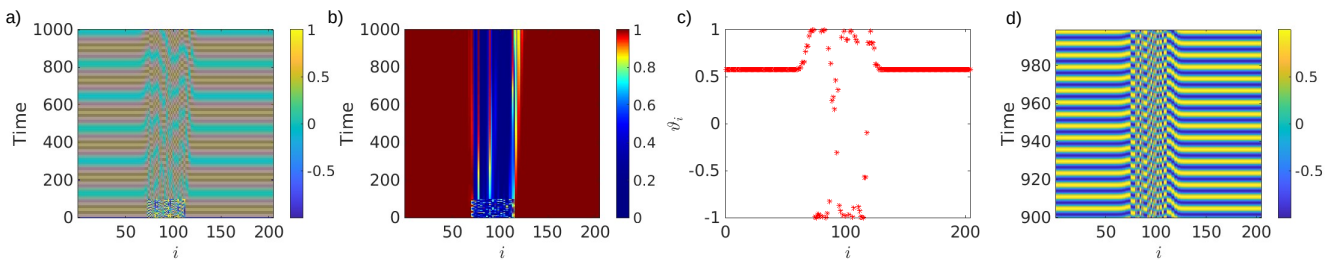


Figure 9. Additive pinning induces phase chimera states for the reduced phase model (17) on a 3-hyperring (i.e., 4-body interactions) of 204 nodes. Panel a) depicts the whole time series of the phases $\vartheta_i(t)$ with $i = 1, \dots, N$, panel b) the hyperedge-based local order parameter, panel c) a snapshot of the phases $\vartheta_i(t)$ with $i = 1, \dots, N$ for $t_{final} = 1000$ time units and panel d) shows a zoom of the time series of the phases $\vartheta_i(t)$ with $i = 1, \dots, N$. The frequency is $\omega = 1$ and the coupling strength is $\varepsilon = 0.01$. Pinning control is applied to $N_p = 40$ consecutive nodes for $t_p = 100$ time units. The parameters λ_{i_p} are the same of Figs. 3 and 4.

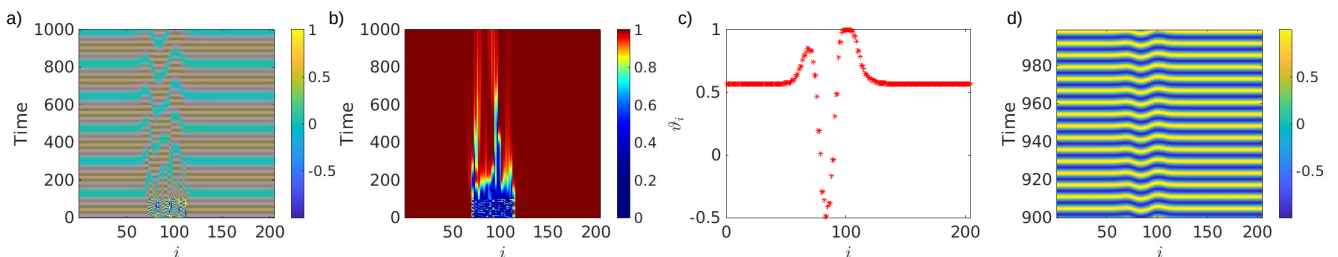


Figure 10. Additive pinning for the reduced phase model (19) on a clique-projected network of 204 nodes. Chimera states do not emerge in this setting, at contrast with the previous Fig. 9. Panel a) depicts the whole time series of the phases $\vartheta_i(t)$ with $i = 1, \dots, N$, panel b) the clique-based local order parameter, panel c) a snapshot of the phases $\vartheta_i(t)$ with $i = 1, \dots, N$ for $t_{final} = 1000$ time units and panel d) shows a zoom of the time series of the phases $\vartheta_i(t)$ with $i = 1, \dots, N$. The frequency is $\omega = 1$ and the coupling strength is $\varepsilon = 0.01$. Pinning control is applied to $N_p = 40$ consecutive nodes for $t_p = 100$ time units. The parameters λ_{i_p} are the same of Figs. 3 and 4.

As a further corroboration of the results shown in this work and of the correctness of our phase reduction approach, let us conclude this section by applying our pinning protocols to the reduced phase models and show that the outcome confirms our claims. We will show the results of additive pinning (10), leaving those for the parametric approach (12) in Appendix C. In Figs. 9 and 10, we show the result of the additive pinning procedure on a 3-hyperring and its corresponding clique-projected network, respectively. The setting is analogous to that of Figs. 3 and 4, and so are the results: while the control induces a chimera state in the higher-order phase reduced model, no chimera emerges in the pairwise setting. The same results are obtained also when performing parametric pinning control (see Appendix C).

V. DISCUSSION

In this work we have shown how pinning control can be applied to higher-order system to trigger the emergence of chimera states and how higher-order interactions are a key feature for the chimera state to develop and persist. It was already known from previous works that higher-order interactions enhanced chimera states, however, the set of parameters, initial conditions and couplings allowing for such behavior remained limited. Thanks to our pinning schemes, that we called additive pinning and parametric pinning, we were able to overcome such limitation and observe chimera patterns for a wide range of settings. Moreover, and this is the most remarkable result, the higher-order framework makes possible to control the presence of chimeras by only acting on a small fraction of the nodes, at striking contrast with the network case, where half of the nodes are to be controlled to achieve this objective. Lastly, our heuristic interpretation of the results goes beyond this work and provides a possible explanation of other previous results regarding synchronization patterns observed in higher-order systems, in particular the claim made by Zhang et al. that higher-order interactions shrink the attraction basin of the synchronized state [85].

Our results clearly show that it is easier and more efficient to trigger the emergence of chimera states when higher-order interactions are present. A further study could be to determine how much energy is needed to control the chimera state in comparison with the pairwise setting, by relying on energy aware controllability measures [86, 87]. Another efficient control strategy could be to apply an intermittent pinning, analogously to the occasional coupling setting developed in the framework of amplitude death [88], where techniques from piecewise-smooth systems could be used [89]. Another interesting direction would be to apply pinning control to directed higher-order structures, such as directed [90] and m -directed hypergraphs [91], which have been proven to greatly affect nonlinear dynamics in the context of synchronization [92] and Turing pattern formation [93], respectively. Pinning approaches in systems with directed higher-order interactions have been developed in some pioneering works [92, 94–96], but not yet in the context of chimera states. Lastly, the recent implementation of higher-order interactions in electric circuits [97] opens the way to further applications in this direction.

In conclusion, this work is one of the first in which tools from control theory are applied to systems with higher-order interactions and it shows the numerous possibilities offered by this novel framework. We believe that there is plenty of exciting research to be done in this direction and that the ground we built with this work is the basis for further studies shedding more light on the interplay between dynamics with higher-order interactions and its control.

Acknowledgements

R.M. and H.N. acknowledge JSPS, Japan KAKENHI JP22K11919, JP22H00516, and JST, Japan CREST JP-MJCR1913 for financial support. The contribution of L.V.G. and M.F. to this work is framed into the activities of the project "CoCoS: Control of Complex Systems", funded by the University of Catania, under the PIA.CE.RI. 2024-26 initiative. We are grateful to Timoteo Carletti for useful discussions, including pointing us to Ref. [75]. R.M. is particularly grateful to Giacomo Baggio and Francesco Lo Iudice for the discussions on pinning control and to Iván León and Yuzuru Kato for the discussions on the phase reduction.

-
- [1] R.M. D'Souza, M. di Bernardo, and Y.Y. Liu, "Controlling complex networks with complex nodes," *Nature Reviews Physics* **5**, 250–262 (2023).
 - [2] A. Sajadi, R.W. Kenyon, and B.M. Hodge, "Synchronization in electric power networks with inherent heterogeneity up to 100% inverter-based renewable generation," *Nature communications* **13**, 2490 (2022).
 - [3] M. Asllani, P. Expert, and T. Carletti, "A minimally invasive neurostimulation method for controlling abnormal synchronisation in the neuronal activity," *PLoS Comput. Biol.* **14**, e1006296 (2018).
 - [4] F. Battiston, G. Cencetti, I. Iacopini, V. Latora, M. Lucas, A. Patania, J.-G. Young, and G. Petri, "Networks beyond pairwise interactions: structure and dynamics," *Phys. Rep.* (2020).
 - [5] F. Battiston, E. Amico, A. Barrat, G. Bianconi, G. Ferraz de Arruda, B. Franceschiello, I. Iacopini, S. Kéfi, V. Latora, Y. Moreno, M.M. Murray, T.P. Peixoto, F. Vaccarino, and G. Petri, "The physics of higher-order interactions in complex systems," *Nat. Phys.* **17**, 1093–1098 (2021).

- [6] G. Bianconi, *Higher-Order Networks: An introduction to simplicial complexes* (Cambridge University Press, 2021).
- [7] S. Boccaletti, P. De Lellis, C.I. Del Genio, K. Alfaro-Bittner, R. Criado, S. Jalan, and M. Romance, “The structure and dynamics of networks with higher order interactions,” *Physics Reports* **1018**, 1–64 (2023).
- [8] C. Bick, E. Gross, H.A. Harrington, and M.T. Schaub, “What are higher-order networks?” *SIAM Review* **65**, 686–731 (2023).
- [9] R.D. Andrew, M. Fagan, B.A. Ballyk, and A.S. Rosen, “Seizure susceptibility and the osmotic state,” *Brain Res.* **498**, 175–180 (2021).
- [10] M. Wang, D. Arteaga, and B.J. He, “Brain mechanisms for simple perception and bistable perception,” *Proc. Natl. Acad. Sci. U.S.A.* **110**, E3350–E3359 (2013).
- [11] G. Petri, P. Expert, F. Turkheimer, R. Carhart-Harris, D. Nutt, P.J. Hellyer, and F. Vaccarino, “Homological scaffolds of brain functional networks,” *J. Royal Soc. Interface* **11**, 20140873 (2014).
- [12] A.E. Sizemore, C. Giusti, A. Kahn, J.M. Vettel, R.F. Betzel, and D.S. Bassett, “Cliques and cavities in the human connectome,” *J. Comp. Neurosci.* **44**, 115–145 (2018).
- [13] J. Grilli, G. Barabás, M.J. Michalska-Smith, and S. Allesina, “Higher-order interactions stabilize dynamics in competitive network models,” *Nature* **548**, 210–213 (2017).
- [14] I. Iacopini, J.R. Foote, N.H. Fefferman, E.P. Derryberry, and M.J. Silk, “Not your private tête-à-tête: leveraging the power of higher-order networks to study animal communication,” *Phil. Trans. R. Soc. Lond. B* **379**, 20230190 (2024).
- [15] D. Centola, J. Becker, D. Brackbill, and A. Baronchelli, “Experimental evidence for tipping points in social convention,” *Science* **360**, 1116–1119 (2018).
- [16] T. Carletti, F. Battiston, G. Cencetti, and D. Fanelli, “Random walks on hypergraphs,” *Phys. Rev. E* **101**, 022308 (2020).
- [17] M.T. Schaub, A.R. Benson, P. Horn, G. Lippner, and A. Jadbabaie, “Random walks on simplicial complexes and the normalized Hodge 1-Laplacian,” *SIAM Rev.* **62**, 353–391 (2020).
- [18] T. Tanaka and T. Aoyagi, “Multistable attractors in a network of phase oscillators with three-body interactions,” *Phys. Rev. Lett.* **106**, 224101 (2011).
- [19] P.S. Skardal and A. Arenas, “Higher-order interactions in complex networks of phase oscillators promote abrupt synchronization switching,” *Comm. Phys.* **3** (2020).
- [20] A.P. Millán, J.J. Torres, and G. Bianconi, “Explosive higher-order Kuramoto dynamics on simplicial complexes,” *Phys. Rev. Lett.* **124**, 218301 (2020).
- [21] I. Iacopini, G. Petri, A. Barrat, and V. Latora, “Simplicial models of social contagion,” *Nat. Comm.* **10**, 2485 (2019).
- [22] T. Carletti, D. Fanelli, and S. Nicoletti, “Dynamical systems on hypergraphs,” *J. phys. Complex.* **1**, 035006 (2020).
- [23] R. Muolo, L. Gallo, V. Latora, M. Frasca, and T. Carletti, “Turing patterns in systems with high-order interaction,” *Chaos Solit. Fractals* **166**, 112912 (2023).
- [24] Y.Y. Liu, J.J. Slotine, and A.L. Barabási, “Controllability of complex networks,” *nature* **473**, 167–173 (2011).
- [25] Y.Y. Liu and A.L. Barabási, “Control principles of complex systems,” *Reviews of Modern Physics* **88**, 035006 (2016).
- [26] Can Chen, Amit Surana, Anthony M Bloch, and Indika Rajapakse, “Controllability of hypergraphs,” *IEEE Transactions on Network Science and Engineering* **8**, 1646–1657 (2021).
- [27] P. De Lellis, F. Della Rossa, F. Lo Iudice, and D. Liuzza, “Pinning control of hypergraphs,” *IEEE Control Systems Letters* **7**, 691–696 (2022).
- [28] P. De Lellis, F. Della Rossa, F. Lo Iudice, and D. Liuzza, “Pinning control of linear systems on hypergraphs,” *European Journal of Control* **74**, 100836 (2023).
- [29] R. Xia and L. Xiang, “Pinning control of simplicial complexes,” *European Journal of Control* **77**, 100994 (2024).
- [30] K. Kaneko, “Clustering, coding, switching, hierarchical ordering, and control in a network of chaotic elements,” *Physica D* **41**, 137–172 (1990).
- [31] V. Hakim and W.J. Rappel, “Dynamics of the globally coupled complex ginzburg-landau equation,” *Physical Review A* **46**, R7347 (1992).
- [32] N. Nakagawa and Y. Kuramoto, “Collective chaos in a population of globally coupled oscillators,” *Progress of Theoretical Physics* **89**, 313–323 (1993).
- [33] M.L. Chabanol, V. Hakim, and W.J. Rappel, “Collective chaos and noise in the globally coupled complex ginzburg-landau equation,” *Physica D: Nonlinear Phenomena* **103**, 273–293 (1997).
- [34] Y. Kuramoto, “Scaling behavior of turbulent oscillators with non-local interaction,” *Prog. Theor. Phys.* **94** (1995).
- [35] Y. Kuramoto and H. Nakao, “Origin of power-law spatial correlations in distributed oscillators and maps with nonlocal coupling,” *Phys. Rev. Lett.* **76** (1996).
- [36] Y. Kuramoto and H. Nakao, “Power-law spatial correlations and the onset of individual motions in self-oscillatory media with non-local coupling,” *Physica D* **103** (1997).
- [37] Y. Kuramoto, D. Battogtokh, and H. Nakao, “Multiaffine chemical turbulence,” *Phys. Rev. Lett.* **81** (1998).
- [38] Y. Kuramoto, H. Nakao, and D. Battogtokh, “Multi-scaled turbulence in large populations of oscillators in a diffusive medium,” *Physica A* **288** (2000).
- [39] Y. Kuramoto and D. Battogtokh, “Coexistence of coherence and incoherence in nonlocally coupled phase oscillators,” *Nonlinear Phenom. Complex Syst.* **5** (2002).
- [40] D.M. Abrams and S.H. Strogatz, “Chimera states for coupled oscillators,” *Phys. Rev. Lett.* **93**, 174102 (2004).
- [41] D. Domínguez and H.A. Cerdeira, “Order and turbulence in rf-driven josephson junction series arrays,” *Phys. Rev. Lett.* **71** (1993).
- [42] L.V. Gambuzza, A. Buscarino, S. Chessa, L. Fortuna, R. Meucci, and M. Frasca, “Experimental investigation of chimera states with quiescent and synchronous domains in coupled electronic oscillators,” *Phys. Rev. E* **9**, 032905 (2014).
- [43] L.V. Gambuzza, L. Minati, and M. Frasca, “Experimental observations of chimera states in locally and non-locally coupled stuart-landau oscillator circuits,” *Chaos, Solitons and Fractals* **138**, 109907 (2020).
- [44] A. M Hagerstrom, T.E. Murphy, R. Roy, P. Hövel, I. Omelchenko, and E. Schöll, “Experimental observation of chimeras in coupled-map lattices,” *Nature Physics* **8**, 658–661 (2012).

- [45] E.A. Martens, S. Thutupalli, A. Fourriere, and O. Hallatschek, “Chimera states in mechanical oscillator networks,” *Proceedings of the National Academy of Sciences* **110**, 10563–10567 (2013).
- [46] M.H. Matheny, J. Emenheiser, W. Fon, A. Chapman, A. Salova, M. Rohden, J. Li, M. Hudoba de Badyn, M. Pósfai, L. Duenas-Osorio, M. Mesbahi, J.P. Crutchfield, M.C. Cross, R.M. D’Souza, and M.L. Roukes, “Exotic states in a simple network of nanoelectromechanical oscillators,” *Science* **363**, eaav7932 (2019).
- [47] T. Chouzouris, I. Omelchenko, A. Zakharova, J. Hlinka, P. Jiruska, and E. Schöll, “Chimera states in brain networks: Empirical neural vs. modular fractal connectivity,” *Chaos* **28**, 045112 (2018).
- [48] S. Majhi, B.K. Bera, D. Ghosh, and M. Perc, “Chimera states in neuronal networks: A review,” *Physics of life reviews* **28**, 100–121 (2019).
- [49] N.C. Rattenborg, C.J. Amlaner, and S.L. Lima, “Behavioral, neurophysiological and evolutionary perspectives on unihemispheric sleep,” *Neuroscience & Biobehavioral Reviews* **24**, 817–842 (2000).
- [50] M. Asllani, B.A. Siebert, A. Arenas, and J.P. Gleeson, “Symmetry-breaking mechanism for the formation of cluster chimera patterns,” *Chaos* **32**, 013107 (2022).
- [51] R. Muolo, J.D. O’Brien, T. Carletti, and M. Asllani, “Persistence of chimera states and the challenge for synchronization in real-world networks,” to appear in *The European Journal of Physics B* (2023).
- [52] A. Zakharova, M. Kapeller, and E. Schöll, “Amplitude chimeras and chimera death in dynamical networks,” in *Journal of Physics: Conference Series*, Vol. 727 (IOP Publishing, 2016) p. 012018.
- [53] E.R. Zajdela and D.M. Abrams, “Phase chimera states: frozen patterns of disorder,” arxiv preprint <https://arxiv.org/abs/2308.06190> (2023).
- [54] A. Zakharova, *Chimera Patterns in Networks. Interplay between Dynamics, Structure, Noise, and Delay* (Springer, 2020).
- [55] F. Parastesh, S. Jafari, H. Azarnoush, Z. Shahriari, Z. Wang, S. Boccaletti, and M. Perc, “Chimeras,” *Physics Reports* **898**, 1–114 (2021).
- [56] S. Kundu and D. Ghosh, “Higher-order interactions promote chimera states,” *Physical Review E* **105**, L042202 (2022).
- [57] X. Li, D. Ghosh, and Y. Lei, “Chimera states in coupled pendulum with higher-order interactions,” *Chaos, Solitons and Fractals* **170**, 113325 (2023).
- [58] C. Bick, T. Böhle, and C. Kuehn, “Phase oscillator networks with nonlocal higher-order interactions: Twisted states, stability, and bifurcations,” *SIAM J. Appl. Dyn. Syst.* **22** (2023).
- [59] R. Muolo, T. Njoungou, L.V. Gambuzza, T. Carletti, and M. Frasca, “Phase chimera states on nonlocal hyperrings,” *Physical Review E* **109**, L022201 (2024).
- [60] R.O. Grigoriev, M.C. Cross, and H.G. Schuster, “Pinning control of spatiotemporal chaos,” *Physical Review Letters* **79**, 2795 (1997).
- [61] F. Sorrentino, M. di Bernardo, F. Garofalo, and G. Chen, “Controllability of complex networks via pinning,” *Physical Review E* **75**, 046103 (2007).
- [62] F. Lo Iudice, F. Garofalo, and P. De Lellis, “Bounded partial pinning control of network dynamical systems,” *IEEE Transactions on Control of Network Systems* **10**, 238–248 (2022).
- [63] C. Ancona, P. De Lellis, and F. Lo Iudice, “Influencing opinions in a nonlinear pinning control model,” *IEEE Control Systems Letters* **7**, 1945–1950 (2023).
- [64] E.F. Du Toit and I.K. Craig, “Selective pinning control of the average disease transmissibility in an hiv contact network,” *Physical Review E* **92**, 012810 (2015).
- [65] P. Yang, Z. Xu, J. Feng, and X. Fu, “Feedback pinning control of collective behaviors aroused by epidemic spread on complex networks,” *Chaos* **29** (2019).
- [66] A. Buscarino, C. Corradino, L. Fortuna, and M. Frasca, “Turing patterns via pinning control in the simplest memristive cellular nonlinear networks,” *Chaos* **29** (2019).
- [67] M. Porfiri and M. di Bernardo, “Criteria for global pinning-controllability of complex networks,” *Automatica* **44**, 3100–3106 (2008).
- [68] W. Yu, G. Chen, J. Lu, and J. Kurths, “Synchronization via pinning control on general complex networks,” *SIAM Journal on Control and Optimization* **51**, 1395–1416 (2013).
- [69] L.V. Gambuzza and M. Frasca, “Pinning control of chimera states,” *Physical Review E* **94**, 022306 (2016).
- [70] H. Nakao, “Phase reduction approach to synchronisation of nonlinear oscillators,” *Contemporary Physics* **57**, 188–214 (2016).
- [71] H. Nakao, “Complex ginzburg-landau equation on networks and its non-uniform dynamics,” *Eur. Phys. J. Spec. Top.* **223**, 2411–2421 (2014).
- [72] L.V. Gambuzza, F. Di Patti, L. Gallo, S. Lepri, M. Romance, R. Criado, M. Frasca, V. Latora, and S. Boccaletti, “Stability of synchronization in simplicial complexes,” *Nat. Comm.* **12**, 1–13 (2021).
- [73] L. Neuhäuser, A.W. Mellor, and R. Lambiotte, “Multibody interactions and nonlinear consensus dynamics on networked systems,” *Phys. Rev. E* **101**, 032310 (2020).
- [74] Y. Kuramoto, “Self-entrainment of a population of coupled non-linear oscillators,” in *International Symposium on Mathematical Problems in Theoretical Physics*, edited by Huzihiro Araki (Springer Berlin Heidelberg, Berlin, Heidelberg, 1975) pp. 420–422.
- [75] M. Shanahan, “Metastable chimera states in community-structured oscillator networks,” *Chaos: An Interdisciplinary Journal of Nonlinear Science* **20** (2010).
- [76] S. Kundu and D. Ghosh, “High-order interactions promote chimera states,” *Physical Review E* **105**, L042202 (2022).
- [77] Y. Kuramoto and H. Nakao, “On the concept of dynamical reduction: the case of coupled oscillators,” *Philosophical Transactions of the Royal Society A* **377**, 20190041 (2019).
- [78] I. León and H. Nakao, “Analytical phase reduction for weakly nonlinear oscillators,” *Chaos, Solitons & Fractals* **176**, 114117 (2023).
- [79] P. Ashwin and A. Rodrigues, “Hopf normal form with sn symmetry and reduction to systems of nonlinearly coupled phase oscillators,” *Physica D: Nonlinear Phenomena* **325**, 14–24 (2016).
- [80] I. León and D. Pazó, “Phase reduction beyond the first order: The case of the mean-field complex ginzburg-landau equation,” *Physical Review E* **100**, 012211 (2019).

- [81] I. León, R. Muolo, S. Hata, and H. Nakao, “Higher-order interactions induce anomalous transitions to synchrony,” *Chaos: An Interdisciplinary Journal of Nonlinear Science* **34** (2024).
- [82] C. Bick, P. Ashwin, and A. Rodrigues, “Chaos in generically coupled phase oscillator networks with nonpairwise interactions,” *Chaos: An Interdisciplinary Journal of Nonlinear Science* **26** (2016).
- [83] P.S. Skardal and A. Arenas, “Abrupt desynchronization and extensive multistability in globally coupled oscillator simplexes,” *Phys. Rev. Lett.* **122**, 248301 (2019).
- [84] Y. Kuramoto, *Chemical oscillations, waves, and turbulence* (Springer-Verlag, New York, 1984).
- [85] Y. Zhang, P.S. Skardal, F. Battiston, G. Petri, and M. Lucas, “Deeper but smaller: Higher-order interactions increase linear stability but shrink basins,” arXiv preprint arXiv:2309.16581 (2023).
- [86] G. Lindmark and C. Altafini, “Minimum energy control for complex networks,” *Scientific reports* **8**, 3188 (2018).
- [87] G. Baggio, F. Pasqualetti, and S. Zampieri, “Energy-aware controllability of complex networks,” *Annual Review of Control, Robotics, and Autonomous Systems* **5**, 465–489 (2022).
- [88] A. Ghosh, S. Mondal, and R.I. Sujith, “Occasional coupling enhances amplitude death in delay-coupled oscillators,” *Chaos: An Interdisciplinary Journal of Nonlinear Science* **32** (2022).
- [89] M. Coraggio, P. De Lellis, and M. di Bernardo, “Convergence and synchronization in networks of piecewise-smooth systems via distributed discontinuous coupling,” *Automatica* **129**, 109596 (2021).
- [90] G. Gallo, G. Longo, S. Pallottino, and S. Nguyen, “Directed hypergraphs and applications,” *Discret. Appl. Math.* **42**, 177–201 (1993).
- [91] L. Gallo, R. Muolo, L.V. Gambuzza, V. Latora, M. Frasca, and T. Carletti, “Synchronization induced by directed higher-order interactions,” *Comm. Phys.* **5** (2022).
- [92] F. Della Rossa, D. Liuzza, F. Lo Iudice, and P. De Lellis, “Emergence and control of synchronization in networks with directed many-body interactions,” *Physical Review Letters* **131**, 207401 (2023).
- [93] M. Dorchain, W. Segnou, R. Muolo, and T. Carletti, “Impact of directionality on the emergence of turing patterns on m-directed higher-order structures,” arXiv preprint <https://arxiv.org/abs/2408.04721> (2024).
- [94] T. Shi, Y. Qin, Q. Yang, Z. Ma, and K. Li, “Synchronization of directed uniform hypergraphs via adaptive pinning control,” *Physica A: Statistical Mechanics and its Applications* **615**, 128571 (2023).
- [95] K. Li, Y. Lin, and J. Wang, “Synchronization of multi-directed hypergraphs via adaptive pinning control,” *Chaos, Solitons & Fractals* **184**, 115000 (2024).
- [96] R. Rizzello and P. De Lellis, “Pinning control in networks of nonidentical systems with many-body interactions,” *IEEE Control Systems Letters* (2024).
- [97] V.P. Vera-Ávila, R.R. Rivera-Durón, M.S. Soriano-García, R. Sevilla-Escoboza, and J.M. Buldú, “Electronic implementation of simplicial complexes,” *Chaos, Solitons & Fractals* **183**, 114915 (2024).

Appendix A: Numerical results for different coupling schemes

In the Main Text, we have considered systems of the form of Eq. (2), where the coupling matrix is $D = \begin{bmatrix} 1 & 0 \\ 1 & 0 \end{bmatrix}$. Let us observe that such setting is the one in which it is easier to observe chimera states induced by the initial conditions. However, through our pinning approach, it is possible to observe chimera states also for different configurations of the coupling. In what follows, we give a brief survey of which configurations yield chimera states, obtained by performing parametric pinning control on a 3-hypergraph of 204 nodes, where the parameters are $\alpha = 1$ and $\omega = 1$, the coupling strength is $\varepsilon = 0.01$, and by pinning $N_p = 18$ nodes spaced every 3 for $t_p = 100$ time units and with the parameters ω_{i_p} drawn from a uniform distribution of the interval [0.5, 2.5]. We have performed 10 simulations for each identical setting except for the parameters ω_{i_p} , which changed at every iteration.

The following coupling configurations always lead to chimera states for the examined range of parameters, couplings and pinning features: $D = \begin{bmatrix} 0 & 0 \\ 0 & 1 \end{bmatrix}$, $\begin{bmatrix} 0 & 1 \\ 0 & 1 \end{bmatrix}$, $\begin{bmatrix} 0 & 1 \\ 1 & 0 \end{bmatrix}$, $\begin{bmatrix} 1 & 1 \\ 0 & 0 \end{bmatrix}$, $\begin{bmatrix} 0 & 0 \\ 1 & 1 \end{bmatrix}$, $\begin{bmatrix} 1 & 1 \\ 0 & 1 \end{bmatrix}$.

The following configurations lead 40% – 60% of times to chimeras, depending on the parameters ω_{i_p} :

$D = \begin{bmatrix} 1 & 0 \\ 0 & 0 \end{bmatrix}$, $\begin{bmatrix} 1 & 0 \\ 0 & 1 \end{bmatrix}$, $\begin{bmatrix} 1 & 1 \\ 1 & 0 \end{bmatrix}$, $\begin{bmatrix} 0 & 1 \\ 1 & 1 \end{bmatrix}$. Despite not being as easy as in the former case, chimera states in the latter can be achieved by increasing the coupling strength, the intensity of the parameters ω_{i_p} , the pinned nodes and the pervasiveness of the pinning (e.g., pinning every node instead of 1 every 3).

The following coupling configurations never lead to chimera states for the examined range of parameters, couplings and pinning features: $D = \begin{bmatrix} 1 & 0 \\ 1 & 1 \end{bmatrix}$, $\begin{bmatrix} 1 & 1 \\ 1 & 1 \end{bmatrix}$.

Particularly interesting are the following coupling configurations: $D = \begin{bmatrix} 0 & 1 \\ 0 & 0 \end{bmatrix}$, $\begin{bmatrix} 0 & 0 \\ 1 & 0 \end{bmatrix}$, where a chimera state emerges, but it is unstable and the incoherence region grows until the whole system develops a fully incoherent state. Moreover, such behavior is independent on the number of pinned nodes and occurs also when only one node is perturbed, which makes this setting interesting for applications in which incoherence needs to be achieved. Let us note that, in this case, higher-order interactions

do not play a role, but the key feature is the coupling configuration. In fact, we obtain the same result in the pairwise setting.

Lastly, let us point out that also different hyperring topologies and the additive pinning configuration lead to analogous behaviors and that no chimera nor incoherent states are observed when the higher-order interactions are "flattened" onto the corresponding clique-projected networks with none of the two pinning approaches. Again, let us stress that all the above does not apply to the coupling configurations leading to full incoherence, namely, $\begin{bmatrix} 0 & 1 \\ 0 & 0 \end{bmatrix}$, $\begin{bmatrix} 0 & 0 \\ 1 & 0 \end{bmatrix}$, whose behavior is determined by the coupling and not by the presence of higher-order interactions. In fact, the same behavior is observed also for pairwise interactions.

Appendix B: Scaling with respect to the number of nodes for the parametric pinning control approach

In this Appendix, we complement the Main Text by showing the results obtained for the case of parametric pinning, which are qualitatively analogous to those of Sec. III obtained through the additive pinning approach, i.e., those on the scaling of the fraction of pinned nodes with respect to the hyperring size. In this setting, we are able to keep the number of pinned nodes constant as we increase the size of the structure. Again, let us stress that the total number of nodes in the hyperring increases, but the number of hyperedges is kept constant.

In Fig. B1, we show the results obtained with such control scheme on d -hyperrings with $d = 3, 4, 5, 6$, i.e., 4-, 5-, 6- and 7-body interactions, where we have fixed the number of hyperedges. Indeed, we can observe that we obtain a chimera state by inducing a large region of incoherence (more than half of the nodes) with a control that involves only a small fraction of the nodes. Moreover, the pinned nodes N_p are kept constant for every structure, meaning that N_p does not scale with the number of nodes, but rather with the number of hyperedges, which allows to control large structures with only a handful of nodes. The parameters ω_{i_p} are the same for all the simulations. The pinned nodes are $\approx 8.8\%$ of the total nodes for the 3-hyperring (panels a) and b)), $\approx 6.6\%$ of the total nodes for the 4-hyperring (panels c) and d)), $\approx 5.3\%$ of the total nodes in the 5-hyperring (panels e) and f)) and $\approx 4.4\%$ of the total nodes in the 6-hyperring (panels g) and h)). In the latter case, the pinning scheme consisting in controlling one every 2 junction nodes does not yield a chimera state, not even with stronger coupling, as shown in Fig. B1g-h), where, moreover, we see that the region of incoherence enlarges. This does not change if we increase the number of pinned nodes, but only if we reduce the gap between them.

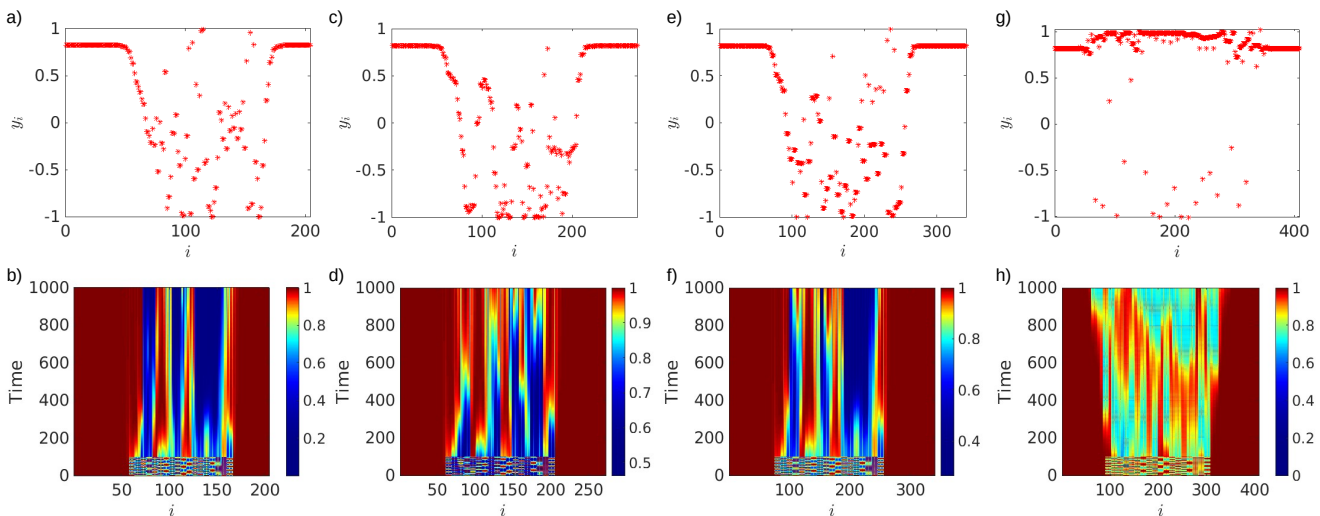


Figure B1. Scaling of the pinned subset with respect to the higher-order structure size with the parametric pinning approach. On the upper panels we depict the snapshots of variables $y_i(t)$ with $i = 1, \dots, N$ for $t_{final} = 1000$ time units, while the lower panels show the hyperedge-based local order parameters. Panels a) and b) report the simulations performed on a 3-hyperring (i.e., 4-body interactions) of 204 nodes, panels c) and d) on a 4-hyperring (i.e., 5-body interactions) of 272 nodes, panels e) and f) on a 5-hyperring (i.e., 6-body interactions) of 340 nodes and panels g) and h) on a 6-hyperring (i.e., 7-body interactions) of 408 nodes. The number of nodes is chosen so that each hyperring is made of 68 hyperedges. Pinning control is applied to $N_p = 18$ nodes as in Fig. 7, i.e., every two junction nodes, to all the structures and for $t_p = 100$ time units. This means that the pinned nodes are $\approx 8.8\%$ of the total nodes in the 3-hyperring, $\approx 6.6\%$ of the total nodes in the 4-hyperring, $\approx 5.3\%$ of the total nodes in the 5-hyperring and $\approx 4.4\%$ of the total nodes in the 6-hyperring. The model parameters are $\alpha = 1$ and $\omega = 1$, the coupling strength is $\varepsilon = 0.01$, except for the 6-hyperring where $\varepsilon = 0.1$, and the parameters ω_{i_p} are drawn from a uniform distribution in the interval $[1.5, 5.5]$ and are the same for all the simulations.

Appendix C: Parametric pinning control of the reduced phase model

In this Appendix, we complement the numerical results of Sec. IV of the Main Text on additive pinning control for the phase reduced model by showing analogous results for the parametric pinning approach. In Figs. C1 and C2, we show the results of the parametric pinning procedure on a 3-hyperherring and its corresponding clique-projected network, respectively. The setting is analogous to that of Figs. 5 and 6 of the Main Text. We see that, while the control induces a chimera state in the higher-order phase reduced model, only a slight incoherence emerges in the pairwise setting, which is not a chimera, as can be seen by looking at the clique-based local order parameter.

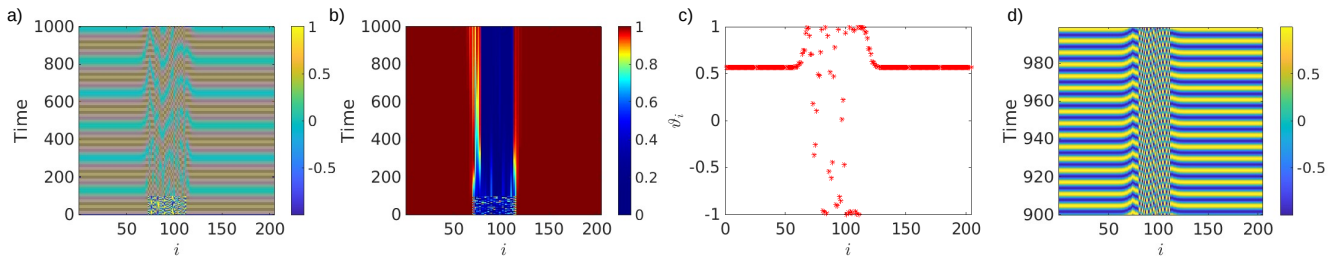


Figure C1. Parametric pinning induces phase chimera states for the reduced phase model (17) of 204 nodes. Panel a) depicts the whole time series of the phases $\vartheta_i(t)$ with $i = 1, \dots, N$, panel b) the hyperedge-based local order parameter, panel c) a snapshot of the phases $\vartheta_i(t)$ with $i = 1, \dots, N$ for $t_{final} = 1000$ time units and panel d) shows a zoom of the time series of the phases $\vartheta_i(t)$ with $i = 1, \dots, N$. The frequency is $\omega = 1$ and the coupling strength is $\varepsilon = 0.01$. Pinning control is applied to $N_p = 40$ consecutive nodes for $t_p = 100$ time units. The parameters ω_{i_p} are the same of Figs. 5 and 6.

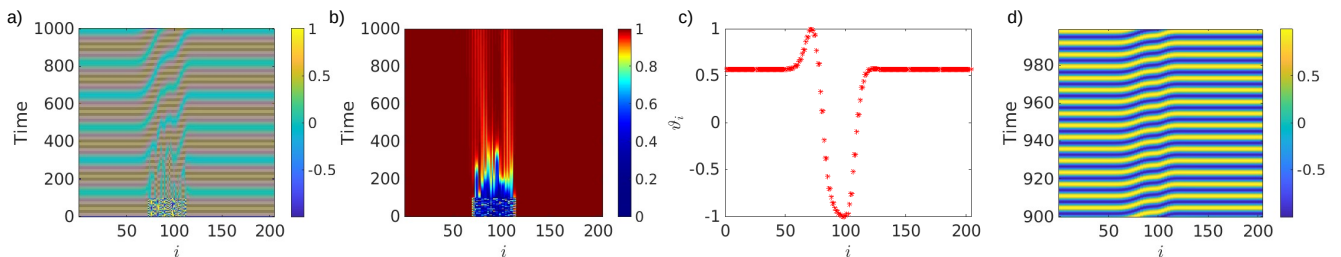


Figure C2. Parametric pinning on a clique-projected network of 204 nodes. Chimera states do not emerge in this setting, at contrast with the previous Fig. C1. Nonetheless, there appears to be a region of weak incoherence, but, as shown by the local order parameter, it is not a chimera because the oscillators remain synchronized with their neighbors. Panel a) depicts the whole time series of the phases $\vartheta_i(t)$ with $i = 1, \dots, N$, panel b) the clique-based local order parameter, panel c) a snapshot of the phases $\vartheta_i(t)$ with $i = 1, \dots, N$ for $t_{final} = 1000$ time units and panel d) shows a zoom of the time series of the phases $\vartheta_i(t)$ with $i = 1, \dots, N$. The model parameters are $\alpha = 1$ and $\omega = 1$ and the coupling strength is $\varepsilon = 0.01$. Pinning control is applied to $N_p = 40$ consecutive nodes for $t_p = 100$ time units. The parameters ω_{i_p} are the same of Figs. 5 and 6.